２．学会発表

・ Hasebe T, Saito T, Yohena S, Kamijo A, Takahashi K, Kuribayashi S, Suzuki T, Tanishita K. In vitro hemodynamic evaluation of inferior vena cava (IVC) filters using particle imaging velocimetry (PIV). Cardiovascular and Interventional Radiological Society of Europe (CIRSE) 2005, Niece, France

・ Saito T, Hasebe T, Yohena S, Matsuoka Y, Kamijo A, Takahashi K, Suzuki T. XPS depth profiling of fluorinated diamond-like carbon film and the inhibition effect of topmost surface fluorine on platelet adhesion and activation. The 10th International Conference on New Diamond Science and Technology (ICNDST-10), Tsukuba, Japan, May11 – 14, 2005

・ Yohena S, T. Hasebe T, Saito T, Matsuoka Y, Kamijo A, Takahashi K, Suzuki T. Platelet adhesion and activation on fluorinated amorphous carbon films. The 10th International Conference on New Diamond Science and Technology (ICNDST-10), Tsukuba, Japan, May 11 – 14, 2005

フッ素添加ダイヤモンドライクカーボン(F-DLC)膜上での白血球付着傾向の評価
吉村泰一, 長谷部光泉, 上條亜紀, 石丸哲也, 吉本幸洋, 饒平名智士, 斉藤俊哉, 堀田篤, 鈴木哲也, 高橋孝喜
第19回ダイヤモンドシンポジウム、大阪府（2005.11.24－11.25）

Diamond-like carbon(DLC)の抗血栓性メカニズムの解明：Transmission electron microscopy(TEM)による試料界面での血小板活性化過程の詳細検討
吉本幸洋, 長谷部光泉, 斉藤俊哉, 饒平名智士, 石丸哲也, 吉村泰一, 堀田篤, 上條亜紀, 高橋孝喜, 鈴木哲也
第19回ダイヤモンドシンポジウム、大阪府（2005.11.24－11.25）学会最優秀ポスター賞

Ｇ：知的財産権の出願・登録状況
該当なし

厚生労働科学研究費補助金（医薬品・医療機器等レギュラトリーサイエンス総合研究事業）

分担研究報告書

臍帯血の供給に関する研究

分担研究者
十字猛夫　日本赤十字社中央研究所長
高梨美乃子　東京都赤十字血液センター技術部長

研究要旨：
臍帯血バンク運営上、提供され調製保存施設に受け入れられる臍帯血のうち50-60％のみが移植用として調製保存される。臍帯血の有効活用のために、移植のための細胞数基準に至らない場合には研究用に活用すべく研究者とのネットワークを構築した。全体の約3割、バンクとしての保存にならない臍帯血のうち約7割を研究用に譲渡することができた。

A：研究目的

臍帯血バンク事業では採取協力施設の妊婦さんらに広く協力を呼びかける一方、実際に移植用としての細胞数基準に達しない臍帯血は凍結保存に至らない。この様な臍帯血をできる限り早く研究者に提供するシステムを構築する。

B：研究方法

臍帯血バンクへの臍帯血提供の同意には、移植に至らない場合の研究用使用も含まれている。ただし移植医療に貢献できる研究でなければならない。東京都赤十字血液センター臍帯血バンクでは、研究用譲渡を希望する研究者から提出された研究計画書、当該施設の倫理委員会での研究承認書類等を臍帯血バンク研究審査部会に回覧し、2/3以上の賛成多数をもって承認とした。あらかじめ承認した研究者に対して、臍帯血が研究用と判断した時点で連絡した。

C：研究結果

臍帯血は容量が十分採取された場合に臍帯血バンクへ搬送される。さらに細胞数が十分あれば移植目的に保存可能と判断して、調製を開始する。保存されたのは受入数607件の55.2％、335件であった。272件の保存にいたらない理由は細胞数不足、クロット、受入までに24時間以上経過、母既往歴、家族歴、調製不良、感染症スクリーニング陽性、英国滞在歴および双胎であった。保存できない臍帯血272件のうち細胞数不足が223件（うち細胞数不足かつクロットが15件）、クロット形成を認める検体が37件であった。2005年10月より臍帯血バンクとして調製開始の細胞数基準を9×10^8にあげた為、保存率は減少し、細胞数不足に該当する臍帯血が前年度同時期の26.8％から36.7％に増加した。クロット形成を認める臍帯血では有核細胞回収率が低い可能性があったが、研究者の希望によっては研究用に提供した。また、この判定は臍帯血採取後24時間以内に行われるため、研究者への譲渡時点では臍帯血は採取後おおよそ24時間内外であった。

2005年4月-2006年1月までの実績を以下に示す。

	臍帯血受入数	調製保存数	受入数－保存数	研究用譲渡数	譲渡先数
4月	56	33	23	19	5
5月	50	28	22	15	5
6月	71	42	29	23	5
7月	68	41	27	19	5
8月	67	36	31	25	4
9月	85	48	37	20	4
10月	52	24	28	23	5
11月	51	23	28	18	5
12月	56	28	28	19	5
1月	51	32	19	16	5
計	607	335	272	197	--

272件中、細胞数不足及びクロット形成のため研究用譲渡になるものが260件、うち197件（利用率75.8％）を研究用に提供することができた。

D：考察

臍帯血が研究用に譲渡できるかは予測が困難である。研究者によっては研究曜日が限られており、指定曜日および前回譲渡からの時間経過を勘案して臍帯血バンクから研究者宛に連絡した。研究用譲渡利用率は昨年と同程度であったが、提供絶対数は前年後同時期の126件より56％増加した。

臍帯血バンク運営効率化の為に細胞数の多い臍帯血のみを保存する方針が全国的にとられており、臍帯血採取に協力頂いても保存となる可能性が下がりつつある。臍帯血バンクに協力する妊産婦の意思を尊重し、産科スタッフの意欲を保つ為にも臍帯血が保存基準に満たない場合には有効活用を図るべきである。臍帯血バンクでも各種調製保存手技のバリデーションのために一部が使用されるが、更に研究にも協力し、よって移植医療に貢献すべきと考える。臍帯血が移植目的に保存されない理由のうちクロットについても、研究によっては活用できる事が分かった。

E：結論

臍帯血バンクの受入臍帯血の内、細胞数基準およびクロットにより保存できない臍帯血を採血後24時間内外で研究用に譲渡する事が可能である。組織的に譲渡対象のうち75.8％を研究者に譲渡した。

F：研究発表

該当なし

G：知的所有権の出願・取得情報

該当なし

Ⅲ．　研究成果の刊行に関する一覧

研究成果の刊行に関する一覧表(論文)

発表者氏名	論文タイトル名	発表誌名	巻名	ページ	出版年
Kawazu M, Asai T, Ichikawa M, Yamamoto G, Saito T, Goyama S, Mitani K, Miyazono K, Chiba S, Ogawa S, Kurokawa M, Hirai H.	Functional domains of Runx1 are differentially required for CD4 repression, TCRb expression, and CD4/8 double-negative to CD4/8 double-positive transition in thymocyte development.	J Immunol	174	3526-3533	2005
Kanda Y, Oshima K, Asano-Mori Y, Kandabashi K, Nakagawa M, Sakata-Yanagimoto M, Izutsu K, Hangaishi A, Tsujino S, Ogawa S, Motokura T, Chiba S, Hirai H.	In vivo alemtuzumab enables haploidentical HLA-mismatched hematopoietic stem cell transplantation without ex vivo graft manipulation.	Transplantation	79	1351-1357	2005
Kanda Y, Komatsu Y, Akahane M, Kojima S, Asano-Mori Y, Tada M, Oshima K, Isayama H, Ogawa S, Motokura T, Chiba S, Ohtomo K, Omata M, Hirai H.	Graft-versus-tumor effect against advanced pancreatic cancer after allogeneic reduced-intensity stem cell transplantation.	Transplantation	79	821-827	2005
Masuda S, Kumano K, Shimizu K, Imai Y, Kurokawa M, Ogawa S, Miyagishi M, Taira K, Hirai H, Chiba S.	The Notch1 oncoprotein antagonizes TGF-β /Smad-mediated cell growth suppression via sequestration of co-activator p300.	Cancer Science	96	74-282	2005
Crcareva A, Saito T, Kunisato A, Kumano K, Suzuki T, Sakata-Yanagimoto M, Kawazu M, Stojanovic A, Kurokawa M, Ogawa S. Chiba S.	Hematopoietic stem cells expanded by fibroblast growth factor-1 are excellent targets for retrovirus-mediated gene delivery.	Exp Hematol	33	1459-1469	2005
Haraguchi K, Takahashi T, Matsumoto A, Asai T, Kanda Y, Kurokawa M, Ogawa S, Oda H, Taniguchi M, Hirai H, Chiba S.	Host-residual invariant NK T cells attenuate graft-versus-host immunity.	J Immunol	175	1320-1328	2005
Lee SY, Kumano K, Masuda S, Hangaishi A, Takita J, Nakazaki K, Kurokawa M, Hayashi Y, Ogawa S, Chiba S.	Mutations of the Notch1 gene in T-cell acute lymphoblastic leukemia: analysis in adults and children.	Leukemia	19	1841-1843	2005
Saeki K, Yasugi E, Okuma E, Breit SN, Nakamura M, Toda T, Kaburagi Y, Yuo A.	Proteomic analysis on insulin signaling in human hematopoietic cells: identification of CLIC1 and SRp20 as novel downstream effectors of insulin.	Am J Physiol EndocrinolMetab	289	E419-E428	2005

研究成果の刊行に関する一覧表(論文)

発表者氏名	論文タイトル名	発表誌名	巻名	ページ	出版年
Hasebe T, Kamijo A, Hotta A, Takahashi K, Suzuki T.	Diamond-like carbon and fluorinated diamond-like carbon films for cardiovascular medical devices.	J Surface Finishing Society Jap	56	897-905	2005
Hasebe T, Matsuoka Y, Kadama H, Saito T, Yohena S, Kamijo A, Shiraga N, Higuchi M, Kuribayashi S, Takahashi K, Suzuki T.	Lubrication performance of diamond-like carbon and fluorinated diamond-like carbon coatings for intravascular guidewires	Diamond and Related Materials	15	129-132	2006
Saito T, Hasebe T, Yohena S, Matsuoka Y, Kamijo A, Takahashi K, Suzuki T.	Antithrombogenicity of fluorinated diamond-like carbon films.	Diamond and Related Materials	14	1116-1119	2005

Ⅳ. 研究成果の刊行物・別刷

Functional Domains of Runx1 Are Differentially Required for CD4 Repression, TCRβ Expression, and CD4/8 Double-Negative to CD4/8 Double-Positive Transition in Thymocyte Development[1]

Masahito Kawazu,*† Takashi Asai,* Motoshi Ichikawa,* Go Yamamoto,* Toshiki Saito,* Susumu Goyama,* Kinuko Mitani,¶ Kohei Miyazono,† Shigeru Chiba,*‡ Seishi Ogawa,*§ Mineo Kurokawa,[2]* and Hisamaru Hirai*‡

Runx1 (AML1) has multiple functions in thymocyte development, including CD4 repression in immature thymocytes, expression of TCRβ, and efficient β-selection. To determine the functional domains of Runx1 important for thymocyte development, we cultured Runx1-deficient murine fetal liver (FL) cells on OP9-Delta-like 1 murine stromal cells, which express Delta-like 1 and support thymocyte development in vitro, and introduced Runx1 or C-terminal-deletion mutants of Runx1 into the FL cells by retrovirus infection. In this system, Runx1-deficient FL cells failed to follow normal thymocyte development, whereas the introduction of Runx1 into the cells was sufficient to produce thymocyte development that was indistinguishable from that in wild-type FL cells. In contrast, Runx1 mutants that lacked the activation domain necessary for initiating gene transcription did not fully restore thymocyte differentiation, in that it neither repressed CD4 expression nor promoted the CD4/8 double-negative to CD4/8 double-positive transition. Although the C-terminal VWRPY motif-deficient mutant of Runx1, which cannot interact with the transcriptional corepressor Transducin-like enhancer of split (TLE), promoted the double-negative to double-positive transition, it did not efficiently repress CD4 expression. These results suggest that the activation domain is essential for Runx1 to establish thymocyte development and that Runx1 has both TLE-dependent and TLE-independent functions in thymocyte development. *The Journal of Immunology,* **2005, 174: 3526–3533.**

Runx1 (also called *AML1*, *Pebpa2b*, or *Cbfa2*) encodes a member of a family of runt transcription factors that was first identified in humans as a gene that is disrupted in t(8;21) acute myeloid leukemia (1). Homozygous disruption of *Runx1* in mice revealed that Runx1 plays an essential role in definitive hematopoiesis (2, 3). Furthermore, it has been suggested from the very beginning of its cloning that Runx1 also plays roles during thymocyte development (4–6). Runx1, together with other cofactors, binds to the enhancers of *TCR*α (7), β (8), γ (9), and δ (10) and activates transcription of these genes. Runx1 is expressed during thymocyte development as demonstrated by Northern blotting, as well as in situ hybridization of mRNA (11, 12). It is mainly expressed in cortical thymocytes (13), and quantitative real-time PCR of reverse-transcribed RNA revealed that Runx1 mRNA is abundant in CD4/CD8 double-negative (DN)[3] thymocytes (14). When Runx1 was overexpressed in thymocytes using a transgenic system, it was shown to induce CD8 single-positive (SP) thymocyte differentiation (15) and to inhibit the differentiation of Th2 effector T cells (16). Recently, we found that T cell-specific disruption of *Runx1* in mice using the *Cre-loxP* recombinase system results in a profound defect in the DN to CD4/8 double-positive (DP) transition,[4] and others also demonstrated that Runx1 actively represses *CD4* expression in DN thymocytes (14). Together, these findings confirm that Runx1 plays an essential role in early thymocyte development. In view of its functions in T cell development, it is noteworthy that the *Runx1* gene is disrupted in t(4;21)(q28;q22) found in T cell acute lymphoblastic leukemia (17, 18).

Runx1 has several distinct domains of defined biochemical functions. The Runt domain mediates both binding to DNA and dimerization with core-binding factor β subunit (4), whereas the activation domain interacts with transcriptional coactivators to upregulate transcription of the target genes (19, 20). Toward the C terminus of the activation domain lies an inhibitory domain that counteracts the effect of the activation domain (21). Furthermore,

Departments of *Hematology and Oncology, †Molecular Pathology, ‡Cell Therapy and Transplantation Medicine, and §Regeneration Medicine for Hematopoiesis, Graduate School of Medicine, University of Tokyo, Tokyo, Japan; and ¶Department of Hematology, Dokkyo University School of Medicine, Tochigi, Japan

Received for publication September 22, 2004. Accepted for publication January 4, 2005.

The costs of publication of this article were defrayed in part by the payment of page charges. This article must therefore be hereby marked *advertisement* in accordance with 18 U.S.C. Section 1734 solely to indicate this fact.

[1] This work was supported in part by Grants-in-Aid for Scientific Research from KAKENHI (14370300, 13218021, 13557080, and 16·61610), Special Coordination Funds for Promoting Science and Technology from the Ministry of Education, Culture, Sports, Science and Technology, the Japanese Government, and Research on Human Genome and Tissue Engineering, Health and Labor Sciences Research Grants from the Ministry of Health, Labour and Welfare of Japan, H14-GENOME-006.

[2] Address correspondence and reprint requests to Dr. Mineo Kurokawa, Department of Hematology and Oncology, Graduate School of Medicine, University of Tokyo, 7-3-1 Hongo, Bunkyo-Ku, Tokyo 113-8655, Japan. E-mail address: kurokawa-tky@umin.ac.jp

[3] Abbreviations used in this paper: DN, double-negative; SP, single-positive; DP, double-positive; TLE, Transducin-like enhancer of split; FTOC, fetal thymus organ culture; FL, fetal liver; tg, transgenic; rh, recombinant human; cko, conditionally knocked out; ctrl, control.

[4] T. Asai, T. Yamagata, T. Saito, M. Ichikawa, S. Seo, G. Yamamoto, K. Maki, K. Mitani, H. Oda, S. Chiba, et al. Runx1 is required for integrity of the pre-T cell receptor complex and Lck kinase activity in early thymocyte development. *Submitted for publication.*

0022-1767/05/$02.00

the C-terminal VWRPY motif, which mediates the interaction with Transducin-like enhancer of split (TLE), a transcriptional corepressor (22, 23) (see Fig. 3*A*), and a domain which represses *p21* transcription through the interaction with mammalian Sim3 isoform A corepressor (24) (not shown in Fig. 3*A*) are also known. Runx1 activates the transcription of different genes by interacting with different cofactors in various types of cells (25). To elucidate the mechanism by which Runx1 exerts various functions, the contributions of each domain to a particular function of Runx1 have been evaluated. Okuda et al. (26) examined the ability of full-length and mutant *Runx1* genes to rescue the hemopoietic defect in Runx1-deficient embryonic stem cells through a knock-in approach and demonstrated that the activation domain, but not the VWRPY motif, is indispensable for definitive hematopoiesis. No alterations in thymocyte subpopulations were detected in mice in which the VWRPY motif of Runx1 is genetically disrupted, although they have a significantly small thymus (27). In their study, the roles of the activation domain during thymocyte development were not assessed, due to a profound defect in hematopoiesis in the absence of the activation domain of Runx1. Therefore, the roles of functional domains of Runx1 in thymocyte development have not yet been adequately clarified.

Although fetal thymus organ culture (FTOC) has been conventionally used for in vitro studies on thymocyte development (28), it is difficult to achieve high gene-transduction efficiency and to obtain a sufficient number of cells for analyses with FTOC. We used an in vitro culture system in which fetal liver (FL) cells from wild-type mouse embryos follow normal thymocyte development on a layer of OP9-Delta-like 1 (DL1) murine stromal cells expressing a Notch ligand, DL1, on their surface (29, 30). In this system, FL cells from Runx1-deficient embryos exhibited defective thymocyte development, which was successfully restored by the reintroduction of full-length Runx1 by retroviral infection. We also introduced several forms of Runx1 mutants into the Runx1-deficient FL cells and evaluated their ability to restore thymocyte development, which revealed distinct functions of Runx1 domains during thymocyte development.

Materials and Methods

Preparation of cDNAs of Runx1 mutants and gene transduction

cDNAs of C-terminal deletion mutants of Runx1, Δ447, Δ372, Δ320, and Δ291, with a *Not*I site on their 5′ terminus and an *Xho*I site on their 3′ terminus, were PCR amplified from template murine *Runx1* cDNA (a gift from M. Satake, Tohoku University, Sendai, Japan) using *TaKaRa LA taq* (Takara Bio) with the following sets of primers: a sense oligonucleotide for all constructs, 5′-AAAAGCGGCCGCATCGATACCATGCGTATCCCC GT-3′; antisense oligonucleotides: Δ*477*, 5′-TTTTCTCGAGTCAGGC CTCCTCCAGGCGCGCGGG-3′; Δ*372*, 5′-TTTTCTCGAGTCAGCCGG TCTGGAAGGGCCCGGC-3′; Δ*320*, 5′-TTTTCTCGAGTCAGCGCGGG TCGGAGATGGACG-3′; and Δ*291*, 5′-TTTTCTCGAGTCAAAGTT CTGCAGAGAGGCTGG-3′. Each PCR product was digested with *Not*I and *Xho*I and cloned into the *Not*I-*Xho*I site, 5′ upstream of internal ribosomal entry site-*GFP* of the *pGCDNsam* (a gift from H. Nakauchi, Tokyo University, Tokyo, Japan) retrovirus vector (31). Nucleotide sequences of these mutant plasmids were confirmed using the ABI Ready Reaction Dye Terminator Cycle Sequencing kit and ABI3100 semiautomated sequencers (Applied Biosystems). To obtain retrovirus-producing cells, ψMP34 packaging cells (a gift from Wakunaga Pharmaceutical) were transfected with these retrovirus plasmids, followed by single cell sorting for GFP with a FACSVantage (BD Biosciences). To characterize cells transduced with retrovirus plasmids, GFP-positive cells were gated and analyzed.

Cell preparation and genotyping

Embryos at 14.5 days postcoitus (E14.5) were obtained by mating *Runx1*$^{+/-}$ mice (female) and *Runx1*$^{floxed/+}$, *Lck-Cre* transgenic (tg)$^{+}$ mice (male), both of which had been backcrossed for nine generations to C57BL/6. *Lck-Cre* tg mice were kindly provided by J. Takeda (Osaka University, Osaka, Japan) (32). FLs were dissected from the E14.5 embryos and then subjected to single cell suspension by pipetting. An aliquot of the FL cell suspension was subjected to DNA extraction followed by genotyping using PCR with primers *f2* (5′-ACAAAACCTAGGTGTAC CAGGAGAACAAGT-3′), *f120* (5′-CCCTGAAGACAGGAGAAGTTT CCA-3′), and *r1* (5′-GTCTACTCCTTGCCTCAGAAAACAAAAAC-3′), in which floxed and floxed-out (or deleted) alleles were amplified as 280-bp (f120-r1) and 220-bp (f2-r1) PCR fragments, respectively.

Culture of FL cells on OP9-DL1 stromal cells

FL cells were cultured on OP9-DL1 cells (generous gifts from J.C. Zúñiga-Pflücker, University of Toronto, Toronto, Canada) (29) according to the original descriptions with minor modifications. In brief, mononuclear cells were separated from a single cell suspension of E14.5 embryos of C57BL/6 mice by centrifugation on a Ficoll-Hypaque (AXIS-SHIELD: Lymphoprep) gradient. A total of 5×10^4 mononuclear cells, without further purification of hemopoietic progenitor cells, was cultured on confluent OP9-DL1 cells in flat-bottom 24-well culture plates with 500 μl of MEM (Invitrogen Life Technologies) supplemented with 20% FCS, penicillin/streptomycin, and 5 ng/ml recombinant human (rh) IL-7 (R&D Systems). After 5 days of culture, 5×10^4 cells were passed onto newly prepared OP9-DL1 cells in the presence of 5 ng/ml rhIL-7, and retrovirus infection was performed using polybrene (final concentration 8 μg/ml), followed by another 5 days of culture. A total of 1×10^5 cells were again passed onto newly prepared OP9-DL1 cells and cultured for another 5 days, but in rhIL-7-free culture medium.

Flow cytometry

Cells were collected from culture plates, suspended in PBS, and then incubated with mAbs for 30 min on ice. If necessary, this was followed by additional incubation with the secondary reagents for another 30 min on ice. After being washed with PBS, cells were analyzed by flow cytometry using a FACSCalibur (BD Biosciences) equipped with CellQuest software. All mAbs and fluorochromes used in flow cytometry were purchased from BD Pharmingen: FITC, PE, PerCP, PerCP-CY5.5, allophycocyanin, or Biotin-conjugated CD3ε (500A2), CD4 (RM4-5), CD8a (53-6.7), CD24 (M1/69), CD25 (PC61), CD44 (IM7), CD45.2 (104), CD45R/B220 (RA3-6B2), CD90.2 (Thy1.2; 52-2.1), or TCRβ (H57-597). Intracellular anti-TCRβ allophycocyanin staining was performed using a BD Cytofix/Cytoperm kit (BD Pharmingen) in accordance with the manufacturer's instructions.

Results

Normal FL cells can differentiate into DN and DP thymocytes on OP9-DL1 cells

The ontogenic profiles of nonpurified FL cells on OP9-DL1 cells were essentially similar to those of purified FL cells for hemopoietic progenitor cells (CD24^{low}, Lin$^-$, Sca-1^{high}, CD117/c-Kit$^+$) (29). Most of the FL cells from wild-type C57BL/6 mouse embryos cultured on OP9-DL1 cells expressed Thy1 without the distinct expression of B220, whereas FL cells cultured on parental OP9 cells did not show a high expression level of Thy1 but had apparently committed to B lymphocytes, as manifested by B220 expression (Fig. 1*A*). After 15 days of culture on OP9-DL1 cells, a considerable number of FL-derived cells became CD4$^+$CD8$^+$ (Fig. 1*B*) and were thought to correspond to CD4/8 DP thymocytes. These CD4$^+$CD8$^+$ cells also expressed TCRβ at a level comparable with that in DP thymocytes in adult thymus (Fig. 1*C*), indicating that the FL cells cultured on OP9-DL1 cells in vitro can follow the normal development of DP thymocytes in the thymus. A small number of SP (i.e., CD4$^+$CD8$^-$ or CD4$^-$CD8$^+$) cells were also observed, but they expressed only intermediate levels of TCRβ on their cell surface (Fig. 1*C*), suggesting that these cells were not as fully mature as the CD4 SP cells or the CD8 SP cells in the thymus. Another prevalent population in the normal FL cell culture on OP9-DL1 cells was CD4$^-$CD8$^-$ cells, which were considered to be reminiscent of CD4/CD8 DN thymocytes. DN thymocytes differentiate through the maturation sequences DN1 (CD44$^+$CD25$^-$), DN2 (CD44$^+$CD25$^+$), DN3 (CD44^{low}CD25$^-$), and DN4 (CD44$^-$CD25$^-$) (33), and each DN fraction was detected in FL-derived CD4$^-$CD8$^-$ cells cultured on OP9-DL1 cells

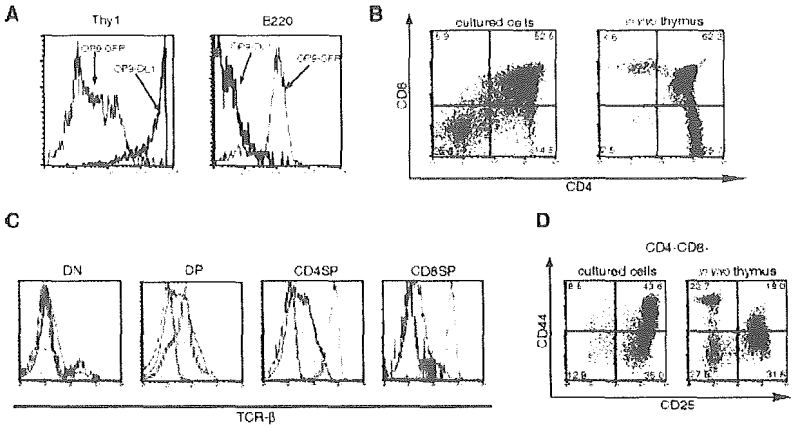

FIGURE 1. FACS analysis of wild-type C57BL/6 FL cells cultured on a stromal layer of OP9 cells that express DL1 (OP9-DL1). *A*, Expression levels of B220 and Thy1 on day 15 in FL cells cultured on an OP9-DL1 layer (thick line) and in FL cells cultured on a control OP9 layer (OP9-GFP; thin line) are shown. Cells were stained with anti-B220 PerCP and anti-Thy1.2 FITC. *B*, CD4/8 expression profile of FL cells cultured on OP9-DL1 for 15 days. The percentage of cells in each quadrant is indicated. *C*, FL cells cultured on OP9-DL1 for 15 days were stained with anti-CD4 PE, anti-CD8 PerCP, and anti-TCRβ allophycocyanin. Expression levels of TCRβ (filled histograms) in each subpopulation, as determined by CD4 and CD8 expression, are shown with the isotype control (blue lines) and expression levels of TCRβ in a corresponding population of adult thymocytes (red lines). *D*, Cells cultured on OP9-DL1 for 15 days were stained with anti-CD4 FITC, anti-CD44 PE, anti-CD8 PerCP, and anti-CD25 allophycocyanin. $CD4^-CD8^-$ cells were gated and their CD25/CD44 expression profile was analyzed. The percentage of cells in each quadrant is indicated.

by staining with CD25 and CD44, although the proportion of cells at the DN2 stage was prominent (Fig. 1*D*).

Phenotypes of Runx1 *conditionally knocked out (cko) FL cells cultured on OP9-DL1 cells*

Using this FL/OP9-DL1 coculture system, FL cells from *Runx1*-targeted (cko: $Runx1^{floxed/-}$, *Lck-Cre* tg) mice were tested for their capacity to differentiate into DP thymocytes. Whereas 10 days of culture of the control (ctrl; $Runx1^{+/+}$, *Lck-Cre* tg) FL cells on OP9-DL1 cells exclusively produced $CD4^-CD8^-$ cells, a similar culture of cko FL cells generated a population that showed an intermediate expression level of CD4 without CD8 ($CD4^{int}CD8^-$) in addition to $CD4^-CD8^-$ cells (Fig. 2*A*). The $CD4^{int}CD8^-$ subset in the cko FL cell culture is thought to be as immature as the $CD4^-CD8^-$ subset because it is quite unlikely that so many cko cells can differentiate beyond DP stage, due to that fact that only a small proportion of ctrl cells progressed to the $CD4^+CD8^+$ cells after 10 days of culture (Fig. 2*A*). Indeed, TCRβ and CD5, whose expression levels rise as thymocytes maturate, were up-regulated in $CD4^+CD8^+$ ctrl cells, but not in $CD4^+CD8^-$ cko cells (Fig. 2*B*). In addition, CD24, whose expression level diminishes as thymocytes maturate, is down-regulated in $CD4^+CD8^+$ ctrl cells, but not in $CD4^+CD8^-$ cko cells (Fig. 2*B*). Furthermore, the expression profile of CD44 and CD25 was comparable with that of $CD4^-CD8^-$ cells (Fig. 2*C*). The extent of Cre-mediated depletion of the floxed *Runx1* allele was greater in $CD4^{int}CD8^-$ cells than in the $CD4^-CD8^-$ cells (Fig. 2*D*), which is consistent with the fact that Runx1 actively represses *CD4* expression in DN thymocytes (14). After 15 days of culture, the ctrl FL cells cultured on OP9-DL1 cells consisted mainly of $CD4^+CD8^+$ and $CD4^-CD8^-$ cells, corresponding to DP and DN thymocytes in the thymus, respectively (Fig. 2*A*). In contrast, cko FL cells cultured for 15 days contained mainly $CD4^-CD8^-$ cells, and only a small fraction were $CD4^+CD8^+$ cells. The $CD4^+CD8^+$ cells from the ctrl FL cell culture showed higher expression levels of TCRβ than did $CD4^-CD8^-$ cells, whereas expression of TCRβ on $CD4^+CD8^+$ cells derived from cko FL cells was as low as that on $CD4^-CD8^-$ cells (data not shown), indicating the impaired maturation of $CD4^+CD8^+$ cells derived from cko FL cells on day 15. These observations are consistent with our unpublished finding in *Runx1* cko mouse, in which TCRβ expression on DP and CD4 SP thymocytes was significantly reduced.[4]

The DN ($CD4^-CD8^-$) population in the ctrl FL-derived cells appeared to contain four subsets of DN1 to DN4 on day 15 of culture (Fig. 2*E*). In contrast, the $CD4^-CD8^-$ population observed in the cko FL cell culture mainly consisted of DN1 and DN2 cells, indicating differentiation arrested at the DN2–3 transition. Thus, on OP9-DL1 cells, ctrl FL cells produced both DN and DP cells in almost the same manner as FL cells from wild-type C57BL/6 mice, whereas thymocyte development from cko FL cells was significantly impaired at the DN2–3 transition and showed the premature expression of CD4.

Runx1 gene transduction can restore the impaired differentiation of Runx1-deficient FL cells

To confirm that the impaired maturation of cko FL-derived cells was caused by a lack of Runx1, we examined whether the reintroduction of Runx1 could rescue the block in the DN2–3 transition found in cko FL-derived cells. The cko FL-derived cells transduced with *Runx1* by retrovirus infection showed a significant increase in DN3 cells accompanied by the appearance of DN4 cells, which was not seen in mock-infected cells (Fig. 3*B*, *top panel*). These results demonstrated that Runx1 is essential for the DN2–3 transition during thymocyte development. Remarkably, when Runx1 was introduced, the control FL cells generated more DN3 and DN4 cells than did mock-infected ctrl FL cells (Fig. 3*B*, *bottom panel*), suggesting that an increased dosage of Runx1 may also affect thymocyte development.

We next sought to determine the functional domains of Runx1 that are involved in thymocyte development. For this purpose, we generated a series of C-terminal deletion mutants of Runx1 (Fig. 3*A*) and transduced them into cko FL cells by retrovirus infection. Infection efficiencies were ~80% as assessed by GFP positivity and were almost constant for all of the constructs (data not shown). Δ447 lacks the C-terminal VWRPY motif, which is required for interaction with TLE (22, 23), whereas Δ372 lacks the inhibitory domain that impedes transcriptional activity mediated by the activation domain of Runx1 (21). The Δ320 mutant lacks a part of the

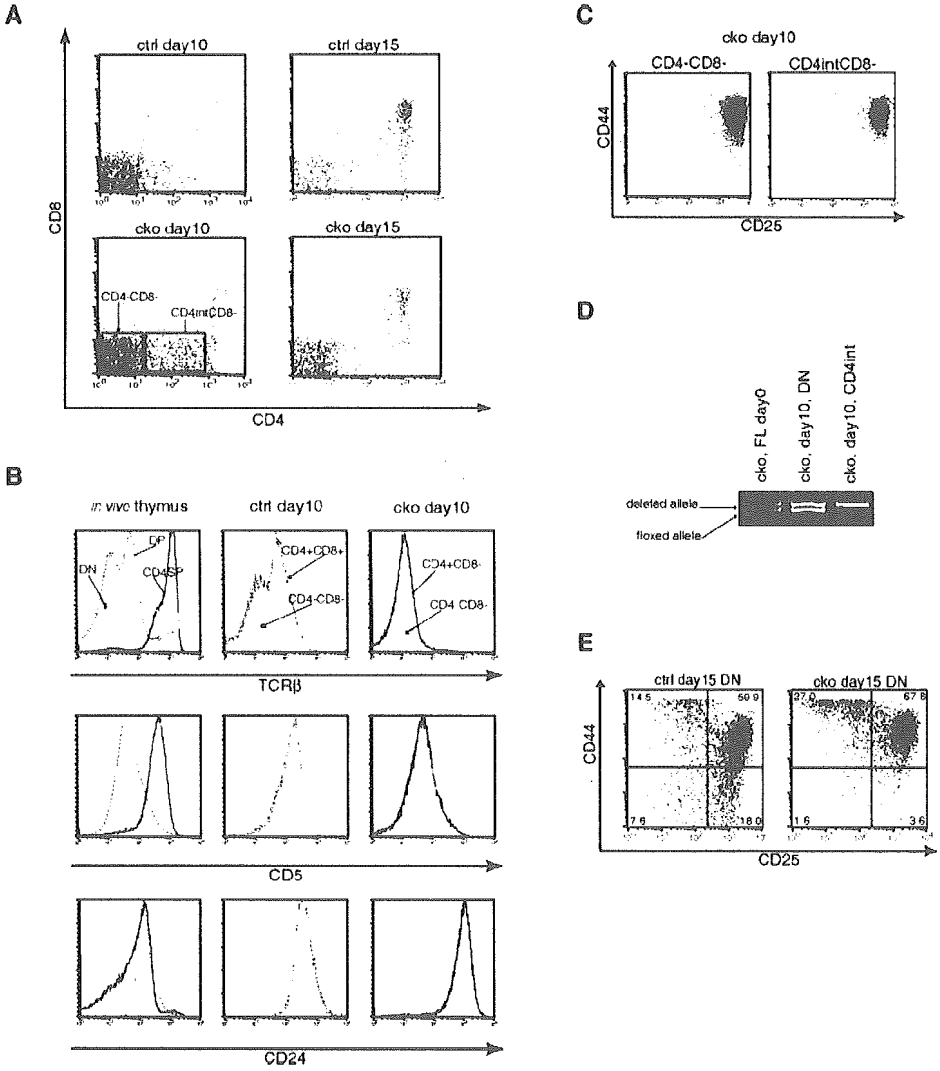

FIGURE 2. FACS analysis of cko FL cells and ctrl FL cells cultured on OP9-DL1. *A*, CD4/CD8 expression profiles of each type of FL-derived cell on days 10 and 15. *B*, Expression levels of TCRβ, CD5, and CD24 in $CD4^+CD8^-$ cko cells (solid lines) and $CD4^+CD8^+$ ctrl cells (dotted lines) cultured for 10 days were compared with those of $CD4^-CD8^-$ cells (gray shades without contour). Those for the indicated subsets of ctrl cells cultured for 10 days and thymocytes derived from adult thymus were also presented. *C*, CD25/CD44 expression profiles of $CD4^-CD8^-$ cells and $CD4^{int}CD8^-$ cells among cko FL cells cultured for 10 days. *D*, Genotype of each subpopulation of cko FL-derived cells, which were sorted with a FACSVantage SE cell sorter (BD Biosciences) after being stained with anti-CD4 PE and anti-CD8 PerCP-CY5.5. Genomic DNA was extracted from sorted cells and electrophoresed after amplification by PCR. *E*, CD25/CD44 expression profiles of $CD4^-CD8^-$ cells on day 15.

activation domain, and Δ291, which completely lacks the activation domain, shows less potent transcriptional activity than does Δ320 (21). The proportions of DN3 and DN4 cells on day 15 of culture were calculated for cko FL-derived cells infected with each mutant (Fig. 3*C*).

Δ*447*-transduced cko FL cells produced DN3 and DN4 cells in numbers comparable with full-length *Runx1*-transduced cko FL cells. Therefore, the VWRPY motif is not necessary for the function of Runx1 in the DN2–3 transition. Although Δ372, which lacks the inhibitory domain, can rescue the DN2–3 transition as efficiently as full-length Runx1, rescue of the DN3–4 transition was still marginally impaired. Despite the fact that the transcriptional activity of Runx1 is derepressed in the absence of the inhibitory domain (21), the differentiation of Δ*372*-transduced cko FL cells is not promoted compared with that of *Runx1*-transduced cko FL cells in this culture system, suggesting that the elevated transcriptional activity does not affect Runx1-dependent thymocyte development.

In contrast, both Δ320 and Δ291, which lack part of and the entire activation domain, respectively, failed to restore either the DN2–3 or DN3–4 transition. Thus, the activation domain is required for the function of Runx1 in the DN2–3 and DN3–4 transitions. Interestingly, the DN3 and DN4 subsets of Δ*320*- or Δ*291*-transduced control FL cells were diminished compared with mock-infected ctrl FL cells (Fig. 3*B*, *bottom panels*), which raises the possibility that both Δ320 and Δ291 suppress the function of endogenous Runx1 in the DN2–3 and DN3–4 transitions in a dominant-negative manner. The suppressive effects of Δ320 and Δ291 were confirmed in three independent experiments (proportions of DN3 cells, $p = 0.031$ for mock vs Δ320 and $p = 0.016$ for mock vs Δ291; proportions of DN4 cells, $p = 0.028$ for mock vs Δ320 and $p = 0.029$ for mock vs Δ291).

To determine the efficiency of Cre-mediated gene deletion in this culture system, genotyping of the *Runx1* alleles was performed for each stage of DN cells. DN3 and DN4 cells were obtained from day 10 culture of *Runx1*-transduced *Runx1*$^{floxed/floxed}$, *Lck-Cre* tg FL cells. The whole culture on day 5 was used to genotype DN2 cells, because almost all of the cells were at the DN2 stage on day 5. Genomic DNA was extracted from each DN subpopulation and used as a template for genotyping. Only the floxed allele was detected in the FL cells on day 0, whereas both the floxed and deleted alleles were detected in day 5 DN2 cells. In contrast, only the deleted allele was detected from the DN3 and DN4 subsets derived from *Runx1*-transduced FL cells (Fig. 3*D*). These results indicated that Cre-mediated gene deletion was only partially achieved in the DN2 cells, but was complete at the DN3 stage in this culture system.

Because our unpublished observation using *Runx1* cko mice revealed decreased TCRβ expression in Runx1-deficient DN3 thymocytes,[4] we examined expression of intracellular TCRβ in DN

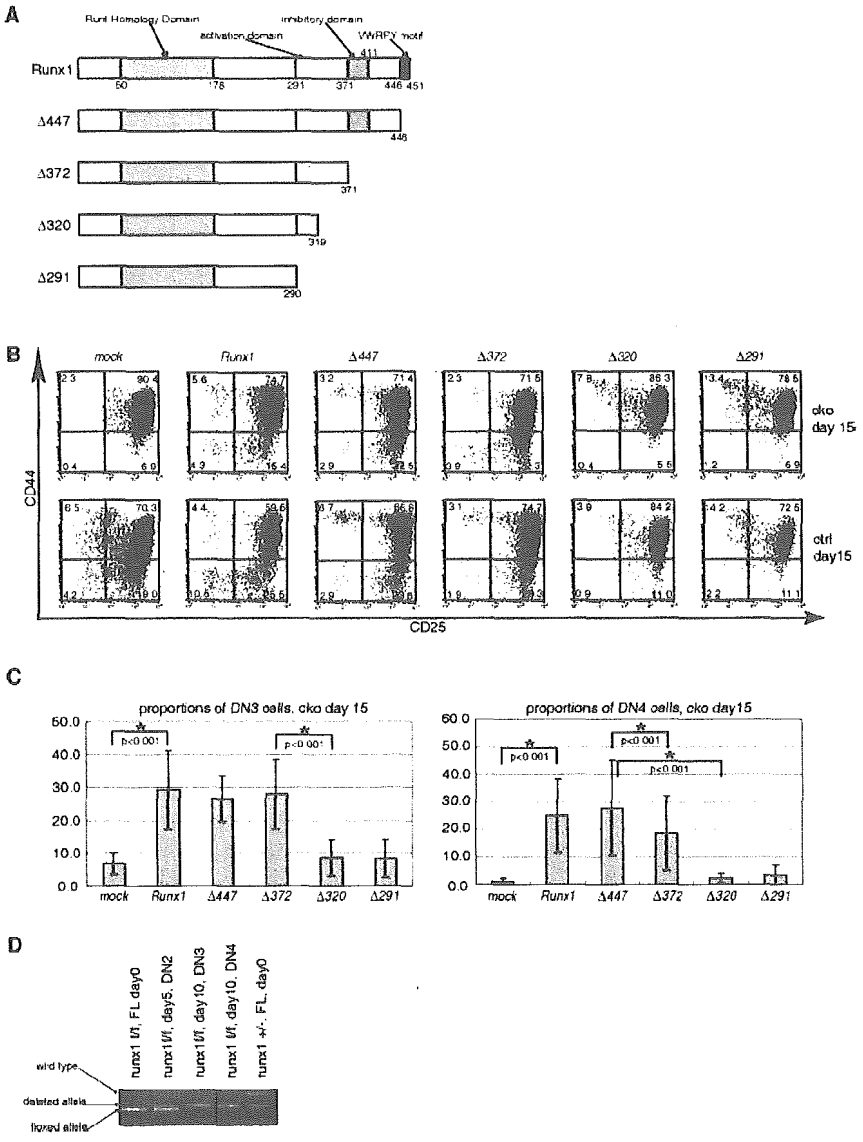

FIGURE 3. Development of DN3 and DN4 cells in FL-derived cells, which were transduced with the genes for Runx1 or its C-terminal deletion mutants. *A*, Construction of Runx1 and C-terminal deletion mutants. Numbers indicate the positions of amino acid residues from the N terminus. *B*, CD25/CD44 expression profile of CD4/CD8 DN cells on day 15 are shown for cko FL-derived cells (*top panels*) and ctrl FL-derived cells (*bottom panels*) with transduced Runx1 mutants. Cells were stained with anti-CD44PE, anti-CD3PerCP, anti-CD4PerCP, anti-CD8 PerCP, and anti-CD25 allophycocyanin. GFP-positive and PerCP-negative cells were gated and analyzed for the CD25/CD44 expression profile. The percentage of cells in each quadrant is indicated. *C*, Proportions (%) of DN3 ($CD44^{low}CD25^{+}$) and DN4 ($CD44^{-}CD25^{-}$) cells on day 15 in nine independent experiments were averaged and are shown with $\pm 1\times$ SE. Asterisks indicate statistically significant differences, and p values were indicated. ANOVA and post hoc comparison (Fisher test) were performed using StatView software (SAS Institute). *D*, DN3 and DN4 thymocytes were sorted by a FACSVantage SE cell sorter (BD Biosciences) after being stained by anti-CD3ε PE, anti-CD4 PE, anti-CD8 PE, anti-CD25 PerCP-CY5.5, and anti-CD44 allophycocyanin. Genomic DNA was extracted from the sorted cells and electrophoresed after PCR amplification.

cells in day 15 culture of FL cells. A significant proportion of *Runx1*-transduced cko DN cells expressed intracellular TCRβ, whereas TCRβ was barely detected in mock-infected cko DN cells (Fig. 4). Transduction of *Δ447* or *Δ372* restored intracellular TCRβ expression to a level comparable with that of full-length *Runx1*, whereas cko DN cells transduced with *Δ320* or *Δ291* did not express intracellular TCRβ. In accordance with the increase in the proportions of DN3 and DN4 cells among *Runx1*-transduced ctrl cells (Fig. 3*B*, *bottom*), the percentage of *Runx1*-transduced ctrl DN cells expressing intracellular TCRβ was increased compared with the

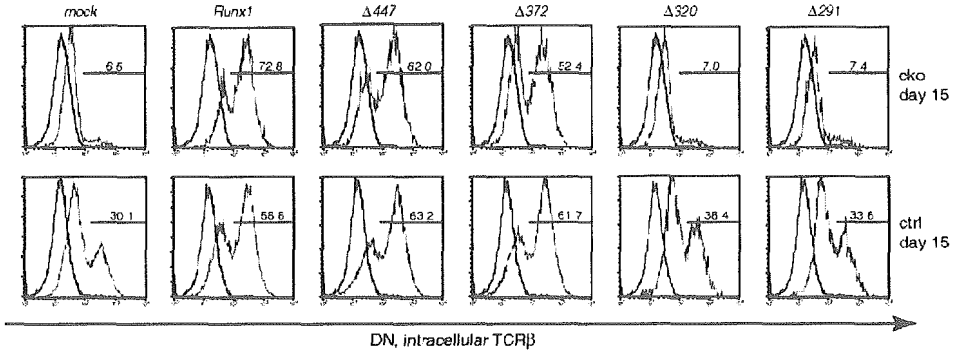

FIGURE 4. Expression levels of intracellular TCRβ in the $CD4^{-}CD8^{-}$ subset among cko (*top panels*) and ctrl (*bottom panels*) FL-derived cells on day 15. Transduced Runx1 mutants are shown above. Cells were stained with anti-CD4 PE, anti-CD8 PerCP, and anti-TCRβ allophycocyanin. GFP-positive, PE-negative, and PerCP-negative cells were analyzed for TCRβ expression (filled histograms). Expression levels of intracellular TCRβ in splenic B cells are overlaid as negative controls (thick lines). The percentages of positive cells are indicated in each histogram.

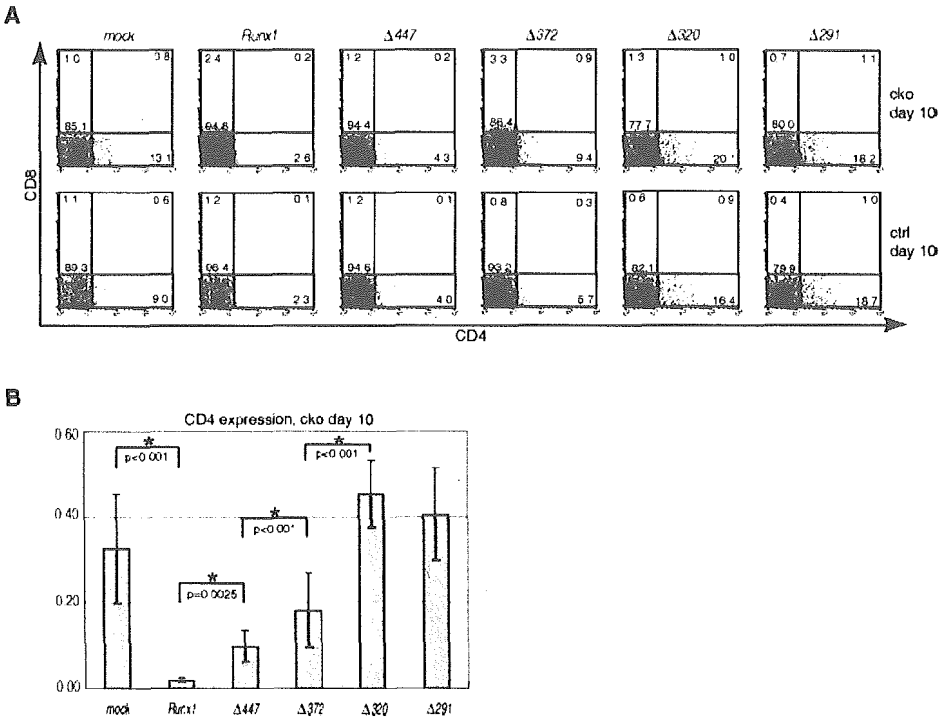

FIGURE 5. CD4 repression in the FL-derived cells transduced with Runx1 or its C-terminal deletion mutants. *A*, $CD4^{-}CD8$ expression profiles of cko (*top panels*) and ctrl (*bottom panels*) FL cells on day 10 of culture. Transduced Runx1 mutants are shown above. Cells were stained with anti-CD4 PE, anti-CD8 PerCP, and anti-CD45.2 allophycocyanin. GFP-positive and allophycocyanin-positive cells were analyzed for CD4/8 expression. The percentage of cells in each quadrant is indicated. *B*, Proportions (%) of $CD4^{int}$ cells among CD8-negative cells in nine independent experiments were averaged and are shown with ±1× SE. ANOVA and post hoc comparison (Fisher test) were performed using StatView software (SAS Institute). Asterisks indicate the statistically significant differences, and *p* values were indicated.

mock-infected cells (Fig. 4, *bottom*), and those TCRβ-expressing cells corresponded with CD44-negative (DN3 or DN4) cells (data not shown). Although it is yet to be determined whether decreased expression of TCRβ was the cause or the result of impaired thymocyte differentiation, the fact that the *TCRβ* gene has canonical binding sites for Runx1 within its enhancer region (34) and is transcriptionally up-regulated by Runx1 (8) supports the notion that Runx1 promotes thymocyte maturation at least partly by up-regulating TCRβ expression. Our results also indicate that the activation domain, but not the VWRPY motif, is critical for Runx1-mediated TCRβ up-regulation.

C-terminal VWRPY motif of Runx1 is necessary for CD4 repression

As shown in Fig. 5*A*, the $CD4^{int}CD8^{-}$ subsets in day 10 culture of cko FL cells disappeared upon the reintroduction of *Runx1* (Fig. 5*A*), which was again consistent with the established role of Runx1 in *CD4* repression (14). This observation also demonstrates that the aberrant expression of CD4 observed in DN subsets of cko FL-derived cells can be ascribed to *Runx1* depletion. To determine the domains of Runx1 that are relevant for CD4 repression, a series of C-terminal deletion mutants of Runx1 were transduced into cko or ctrl FL cells, and the proportion of $CD4^{int}CD8^{-}$ cells was evaluated on day 10 of culture (Fig. 5). Whereas full-length Runx1 almost completely repressed aberrant CD4 expression, only partial repression was seen with Δ447 or Δ372 mutants. These results suggest that CD4 repression by Runx1 requires some C terminus-mediated interaction with other molecules such as TLE. The extent of CD4 repression by Δ447 is greater than that by Δ372, which might reflect the existence of an additional repression domain in the C terminus other than the VWRPY motif (23).

Δ320 and Δ291 each failed to repress CD4 expression, resulting in an increase in the $CD4^{int}$ population compared with the mock-infected cko FL cells. Because *Runx1* depletion is incomplete in the DN subsets of cko FL-derived cells on day 10 (Fig. 2*D*), the increase in the $CD4^{int}$ population is probably due to a dominant-negative effect of Δ320 and Δ291 on remaining endogenous Runx1. This notion is supported by the observation that *Δ320*- or *Δ291*-transduced control FL cells produced a significant number of $CD4^{int}CD8^{-}$ cells, which were barely detected in mock-infected ctrl FL-derived cells (Fig. 5*A*, *bottom*).

Discussion

In the current study, we demonstrated that Runx1 was important for thymocyte development using the FL/OP9-DL1 coculture system. This system is superior to conventional FTOC in that a sufficient number of cells for extensive analyses can be easily obtained, especially DN thymocytes. Another advantage of this system is the highly efficient transfer of the genes of interest. In this study, we were able to introduce various mutants of Runx1 by retroviral infection with an efficiency of ~80% (data not shown), which is higher than that obtained with FTOC. In contrast, terminal maturation of SP cells cannot be achieved in this culture system, which makes it difficult to analyze more mature stages of thymocytes.

The absolute need for Runx1 in thymocyte development in vivo has been unequivocally demonstrated using conditionally *Runx1*-targeted mice. When Runx1-deficient bone marrow cells are transplanted to lethally irradiated mice, the development of thymocytes is severely blocked at the DN2–3 transition (35), whereas the deletion of *Runx1* in later stages of DN thymocytes using the *Lck-Cre* tg results in a profound defect in the DN3–4 transition.[4] Together, these findings suggest that Runx1 is necessary for normal thymocyte development at multiple steps during the DN-DP transition. Despite the DN3–4 block in T lymphocyte-specific *Runx1*-targeted mice, thymocyte development of the cognate FL cells was arrested at the DN2–3 transition in this culture system. The difference in the DN stage at which the developmental block occurs may be due to earlier Cre-mediated *Runx1* deletion in vitro rather than in vivo. In the FL culture system, deletion of the floxed *Runx1* allele occurs predominantly at the DN2–3 transition, which leaves few, if any, DN3 cells with an intact *Runx1* allele (Fig. 3*D*, *lane 3*). *Lck-Cre* tg mice harbor a transgenic gene encoding Cre recombinase driven by the $p56^{lck}$ proximal promoter (32, 36). The *Lck*

encodes a lymphocyte-specific protein tyrosine kinase, which mediates β-chain-dependent signaling during β-selection, is associated with allelic exclusion of β locus (37), and is transcribed from two developmentally regulated, independently functioning promoters. The proximal promoter is used exclusively in thymocytes, but not in peripheral T lymphocytes (38), and Cre-mediated gene deletions are expected to be activated by $p56^{lck}$ proximal promoter at the DN2 and DN3 stages when Vβ gene rearrangement and subsequent β-selection occurs. However, even if the same $p56^{lck}$ proximal promoter is used, exact timing of gene expression differs depending on the transgenic mice lines, and different lines of *Lck-Cre* tg mice are used to target a gene at different developmental stages (39).

The function of the VWRPY motif in hematopoiesis has been examined in embryonic stem cell culture (26) and in para-aortic splanchnopleural culture (40). Because Runx1 mutants that lack the VWRPY motif could fully restore hematopoiesis in Runx1-deficient cells in these two studies, the VWRPY motif does not seem to be necessary for hematopoiesis. On the contrary, because mice in which cDNA for the VWRPY-deficient Runx1 mutant had been homozygously knocked-in to the *Runx1* alleles exhibited a reduced number of thymocytes and deviant CD4 expression during thymocyte ontogeny (27), the VWRPY motif seems to play a role in thymocyte development, although the precise molecular mechanism is unclear. In the present study, although the VWRPY-deficient Runx1 mutant (Δ447) could restore not only maturation to the DN4 subset but also TCRβ expression in cko FL-derived thymocytes as efficiently as wild-type Runx1 (Fig. 4), it had only a limited capacity to repress aberrant CD4 expression (Fig. 5). These different requirements for the VWRPY motif indicate that Runx1 functions in both TLE-dependent and TLE-independent manners during early thymocyte development. In fact, the context-dependent need for interaction with a transcriptional corepressor has been reported for Runt and Groucho, *Drosophila* homologues of Runx and TLE, respectively (41). One possible explanation for TLE-dependent *CD4* repression is that TLE actively converts Runx1 to a transcriptional repressor by recruiting histone deacetylase, as seen in *Drosophila* (41). Another possibility is that TLE displaces some coactivators from Runx1 under particular conditions, which prevents Runx1 from up-regulating *CD4* expression. A similar mechanism has been proposed for transcription by lymphoid enhancer binding protein 1/T cell factor, which is repressed until TLE is replaced by β-catenin (42). Further analyses are needed to clarify the role of the VWRPY motif in the regulation of *CD4* transcription.

The introduction of Runx1 mutants into cko FL cells has shown that the activation domain makes a critical contribution to various functions of Runx1 in thymocyte development, including *CD4* repression, the DN2–3 transition, and the expression of TCRβ. Significantly, Δ320 and Δ291, both of which lack the activation domain, dominantly suppress *CD4* repression and the DN2–3 transition but do not interfere with TCRβ expression. This may be due to a higher affinity of Runx1 for the *TCRβ* enhancer compared with Δ320 and Δ291. Although this speculation is not supported by experimental evidence, a potential mechanism that accounts for this finding is that the interaction of Runx1 with other transcription factors may confer on Runx1 a higher affinity for specific gene promoters. Otherwise, Δ320 and Δ291 may retain a marginal potential to up-regulate TCRβ, which would prevent the total loss of TCRβ when they are forcibly expressed.

In conclusion, we have successfully reproduced the phenotype of Runx1-deficient thymocytes in vitro using the FL/OP9-DL1 coculture system and have evaluated the function of Runx1 and its mutants by retroviral gene transduction. The activation domain is essential for the function of Runx1 in *CD4* repression, the DN2–3 transition, and the expression of TCRβ, whereas the VWRPY motif does not contribute to the DN2–3 transition or the expression of TCRβ, but it is partially involved in *CD4* repression. Further studies are needed to understand how the VWRPY motif of Runx1 regulates *CD4* transcription and how Runx1 functions at multiple steps in thymocyte development.

Acknowledgments

We thank M. Satake for the gift of cDNA for murine *Runx1*, J.C. Zúñiga-Pflücker for OP9-DL1 stromal cells, H. Nakauchi for *pGCDNsam*, and Wakunaga Pharmaceutical for ψMP34 packaging cells. We also thank E. Nakagami-Yamaguchi and T. Yamagata for their helpful discussions.

Disclosures

The authors have no financial conflict of interest

References

1. Miyoshi, H., K. Shimizu, T. Kozu, N. Maseki, Y. Kaneko, and M. Ohki. 1991. t(8;21) breakpoints on chromosome 21 in acute myeloid leukemia are clustered within a limited region of a single gene, AML1. *Proc. Natl. Acad. Sci. USA 88:10431.*
2. Okuda, T., J. van Deursen, S. W. Hiebert, G. Grosveld, and J. R. Downing. 1996. AML1, the target of multiple chromosomal translocations in human leukemia, is essential for normal fetal liver hematopoiesis. *Cell 84:321.*
3. Wang, Q., T. Stacy, M. Binder, M. Marin-Padilla, A. H. Sharpe, and N. A. Speck. 1996. Disruption of the *Cbfa2* gene causes necrosis and hemorrhaging in the central nervous system and blocks definitive hematopoiesis. *Proc. Natl. Acad. Sci. USA 93:3444.*
4. Wang, S., Q. Wang, B. E. Crute, I. N. Melnikova, S. R. Keller, and N. A. Speck. 1993. Cloning and characterization of subunits of the T-cell receptor and murine leukemia virus enhancer core-binding factor. *Mol. Cell. Biol. 13:3324.*
5. Bae, S. C., Y. Yamaguchi-Iwai, E. Ogawa, M. Maruyama, M. Inuzuka, H. Kagoshima, K. Shigesada, M. Satake, and Y. Ito. 1993. Isolation of PEBP2 αB cDNA representing the mouse homolog of human acute myeloid leukemia gene, AML1. *Oncogene 8:809.*
6. Ogawa, E., M. Maruyama, H. Kagoshima, M. Inuzuka, J. Lu, M. Satake, K. Shigesada, and Y. Ito. 1993. PEBP2/PEA2 represents a family of transcription factors homologous to the products of the Drosophila runt gene and the human AML1 gene. *Proc. Natl. Acad. Sci. USA 90:6859.*
7. Giese, K., C. Kingsley, J. R. Kirshner, and R. Grosschedl. 1995. Assembly and function of a TCRα enhancer complex is dependent on LEF-1-induced DNA bending and multiple protein-protein interactions. *Genes Dev. 9:995.*
8. Sun, W., B. J. Graves, and N. A. Speck. 1995. Transactivation of the Moloney murine leukemia virus and T-cell receptor β-chain enhancers by cbf and ets requires intact binding sites for both proteins. *J. Virol. 69:4941.*
9. Hernandez-Munain, C., and M. S. Krangel. 1995. c-Myb and core-binding factor/PEBP2 display functional synergy but bind independently to adjacent sites in the T-cell receptor δ enhancer. *Mol. Cell. Biol. 15:3090.*
10. Hernandez-Munain, C., and M. S. Krangel. 1994. Regulation of the T-cell receptor δ enhancer by functional cooperation between c-Myb and core-binding factors. *Mol. Cell. Biol. 14:473.*
11. Satake, M., S. Nomura, Y. Yamaguchi-Iwai, Y. Takahama, Y. Hashimoto, M. Niki, Y. Kitamura, and Y. Ito. 1995. Expression of the Runt domain-encoding PEBP2 α genes in T cells during thymic development. *Mol. Cell. Biol. 15:1662.*
12. Simeone, A., A. Daga, and F. Calabi. 1995. Expression of runt in the mouse embryo. *Dev. Dyn. 203:61.*
13. Woolf, E., C. Xiao, O. Fainaru, J. Lotem, D. Rosen, V. Negreanu, Y. Bernstein, D. Goldenberg, O. Brenner, G. Berke, D. Levanon, and Y. Groner. 2003. Runx3 and Runx1 are required for CD8 T cell development during thymopoiesis. *Proc. Natl. Acad. Sci. USA 100:7731.*
14. Taniuchi, I., M. Osato, T. Egawa, M. J. Sunshine, S. C. Bae, T. Komori, Y. Ito, and D. R. Littman. 2002. Differential requirements for Runx proteins in CD4 repression and epigenetic silencing during T lymphocyte development. *Cell 111:621.*
15. Hayashi, K., N. Abe, T. Watanabe, M. Obinata, M. Ito, T. Sato, S. Habu, and M. Satake. 2001. Overexpression of AML1 transcription factor drives thymocytes into the CD8 single-positive lineage. *J. Immunol. 167:4957.*
16. Komine, O., K. Hayashi, W. Natsume, T. Watanabe, Y. Seki, N. Seki, R. Yagi, W. Sukzuki, H. Tamauchi, K. Hozumi, et al. 2003. The Runx1 transcription factor inhibits the differentiation of naive $CD4^+$ T cells into the Th2 lineage by repressing GATA3 expression. *J. Exp. Med. 198:51.*
17. Mikhail, F. M., K. A. Serry, N. Hatem, Z. I. Mourad, H. M. Farawela, D. M. El Kaffash, L. Coignet, and G. Nucifora. 2002. A new translocation that rearranges the AML1 gene in a patient with T-cell acute lymphoblastic leukemia. *Cancer Genet. Cytogenet. 135:96.*
18. Mikhail, F. M., L. Coignet, N. Hatem, Z. I. Mourad, H. M. Farawela, D. M. El Kaffash, N. Farahat, and G. Nucifora. 2004. A novel gene, FGA7, is fused to RUNX1/AML1 in a t(4;21)(q28;q22) in a patient with T-cell acute lymphoblastic leukemia. *Genes Chromosomes Cancer 39:110.*
19. Bae, S. C., E. Ogawa, M. Maruyama, H. Oka, M. Satake, K. Shigesada, N. A. Jenkins, D. J. Gilbert, N. G. Copeland, and Y. Ito. 1994. PEBP2 αB/mouse

AML1 consists of multiple isoforms that possess differential transactivation potentials. *Mol. Cell. Biol. 14:3242.*

20. Tanaka, T., K. Tanaka, S. Ogawa, M. Kurokawa, K. Mitani, J. Nishida, Y. Shibata, Y. Yazaki, and H. Hirai. 1995. An acute myeloid leukemia gene, AML1, regulates hemopoietic myeloid cell differentiation and transcriptional activation antagonistically by two alternative spliced forms. *EMBO J. 14:341.*
21. Kanno, T., Y. Kanno, L. F. Chen, E. Ogawa, W. Y. Kim, and Y. Ito. 1998. Intrinsic transcriptional activation-inhibition domains of the polyomavirus enhancer binding protein 2/core binding factor α subunit revealed in the presence of the β subunit. *Mol. Cell. Biol. 18:2444.*
22. Imai, Y., M. Kurokawa, K. Tanaka, A. D. Friedman, S. Ogawa, K. Mitani, Y. Yazaki, and H. Hirai. 1998. TLE, the human homolog of groucho, interacts with AML1 and acts as a repressor of AML1-induced transactivation. *Biochem. Biophys. Res. Commun. 252:582.*
23. Levanon, D., R. E. Goldstein, Y. Bernstein, H. Tang, D. Goldenberg, S. Stifani, Z. Paroush, and Y. Groner. 1998. Transcriptional repression by AML1 and LEF-1 is mediated by the TLE/Groucho corepressors. *Proc. Natl. Acad. Sci. USA 95:11590.*
24. Lutterbach, B., J. J. Westendorf, B. Linggi, S. Isaac, E. Seto, and S. W. Hiebert. 2000. A mechanism of repression by acute myeloid leukemia-1, the target of multiple chromosomal translocations in acute leukemia. *J. Biol. Chem. 275:651.*
25. Kitabayashi, I., A. Yokoyama, K. Shimizu, and M. Ohki. 1998. Interaction and functional cooperation of the leukemia-associated factors AML1 and p300 in myeloid cell differentiation. *EMBO J. 17:2994.*
26. Okuda, T., K. Takeda, Y. Fujita, M. Nishimura, S. Yagyu, M. Yoshida, S. Akira, J. R. Downing, and T. Abe. 2000. Biological characteristics of the leukemia-associated transcriptional factor AML1 disclosed by hematopoietic rescue of AML1-deficient embryonic stem cells by using a knock-in strategy. *Mol. Cell. Biol. 20:319.*
27. Nishimura, M., Y. Fukushima-Nakase, Y. Fujita, M. Nakao, S. Toda, N. Kitamura, T. Abe, and T. Okuda. 2004. VWRPY motif-dependent and -independent roles of AML1/Runx1 transcription factor in murine hematopoietic development. *Blood 103:562.*
28. Kingston, R., E. J. Jenkinson, and J. J. Owen. 1985. A single stem cell can recolonize an embryonic thymus, producing phenotypically distinct T-cell populations. *Nature 317:811.*
29. Schmitt, T. M., and J. C. Zúñiga-Pflücker. 2002. Induction of T cell development from hematopoietic progenitor cells by δ-like-1 in vitro. *Immunity 17:749.*
30. Huang, E. Y., A. M. Gallegos, S. M. Richards, S. M. Lehar, and M. J. Bevan. 2003. Surface expression of Notch1 on thymocytes: correlation with the double-negative to double-positive transition. *J. Immunol. 171:2296.*
31. Suzuki, A., K. Obi, T. Urabe, H. Hayakawa, M. Yamada, S. Kaneko, M. Onodera, Y. Mizuno, and H. Mochizuki. 2002. Feasibility of ex vivo gene therapy for neurological disorders using the new retroviral vector GCDNsap packaged in the vesicular stomatitis virus G protein. *J. Neurochem. 82:953.*
32. Takahama, Y., K. Ohishi, Y. Tokoro, T. Sugawara, Y. Yoshimura, M. Okabe, T. Kinoshita, and J. Takeda. 1998. Functional competence of T cells in the absence of glycosylphosphatidylinositol-anchored proteins caused by T cell-specific disruption of the Pig-a gene. *Eur. J. Immunol. 28:2159.*
33. Godfrey, D. I., J. Kennedy, T. Suda, and A. Zlotnik. 1993. A developmental pathway involving four phenotypically and functionally distinct subsets of $CD3^-CD4^-CD8^-$ triple-negative adult mouse thymocytes defined by CD44 and CD25 expression. *J. Immunol. 150:4244.*
34. Krimpenfort, P., R. de Jong, Y. Uematsu, Z. Dembic, S. Ryser, H. von Boehmer, M. Steinmetz, and A. Berns. 1988. Transcription of T cell receptor β-chain genes is controlled by a downstream regulatory element. *EMBO J. 7:745.*
35. Ichikawa, M., T. Asai, T. Saito, G. Yamamoto, S. Seo, I. Yamazaki, T. Yamagata, K. Mitani, S. Chiba, H. Hirai, S. Ogawa, and M. Kurokawa. 2004. AML-1 is required for megakaryocytic maturation and lymphocytic differentiation, but not for maintenance of hematopoietic stem cells in adult hematopoiesis. [Published erratum appears in *2005 Nat. Med. 11:102.*] *Nat. Med. 10:299.*
36. Hennet, T., F. K. Hagen, L. A. Tabak, and J. D. Marth. 1995. T-cell-specific deletion of a polypeptide *N*-acetylgalactosaminyl-transferase gene by site-directed recombination. *Proc. Natl. Acad. Sci. USA 92:12070.*
37. Anderson, S. J., and R. M. Perlmutter. 1995. A signaling pathway governing early thymocyte maturation. *Immunol. Today 16:99.*
38. Allen, J. M., K. A. Forbush, and R. M. Perlmutter. 1992. Functional dissection of the lck proximal promoter. *Mol. Cell. Biol. 12:2758.*
39. Bender, T. P., C. S. Kremer, M. Kraus, T. Buch, and K. Rajewsky. 2004. Critical functions for c-Myb at three checkpoints during thymocyte development. *Nat. Immunol. 5:721.*
40. Goyama, S., Y. Yamaguchi, Y. Imai, M. Kawazu, M. Nakagawa, T. Asai, K. Kumano, K. Mitani, S. Ogawa, S. Chiba, M. Kurokawa, and H. Hirai. 2004. The transcriptionally active form of AML1 is required for hematopoietic rescue of the AML1-deficient embryonic para-aortic splanchnopleural (P-Sp) region. *Blood 104:3558.*
41. Wheeler, J. C., C. VanderZwan, X. Xu, D. Swantek, W. D. Tracey, and J. P. Gergen. 2002. Distinct in vivo requirements for establishment versus maintenance of transcriptional repression. *Nat. Genet. 32:206.*
42. Roose, J., M. Molenaar, J. Peterson, J. Hurenkamp, H. Brantjes, P. Moerer, M. van de Wetering, O. Destree, and H. Clevers. 1998. The Xenopus Wnt effector XTcf-3 interacts with Groucho-related transcriptional repressors. *Nature 395:608.*

In Vivo Alemtuzumab Enables Haploidentical Human Leukocyte Antigen-Mismatched Hematopoietic Stem-Cell Transplantation Without Ex Vivo Graft Manipulation

Yoshinobu Kanda, Kumi Oshima, Yuki Asano-Mori, Koji Kandabashi, Masahiro Nakagawa, Mamiko Sakata-Yanagimoto, Koji Izutsu, Akira Hangaishi, Shiho Tsujino, Seishi Ogawa, Toru Motokura, Shigeru Chiba, and Hisamaru Hirai

Background. Alemtuzumab, a humanized monoclonal antibody directed against human CD52, has a strong lympholytic effect. This study evaluates the safety of unmanipulated peripheral blood stem-cell transplantation from two or three loci-mismatched related donors using alemtuzumab in vivo.

Methods. A total body irradiation-based regimen was used in young patients, whereas those 50 years or older received fludarabine-based conditioning. Alemtuzumab was added to these regimens by intravenous infusion at 0.2 mg/kg per day for 6 days (days −8 to −3).

Results. We treated 12 patients with a median age of 49.5 years. Eight patients demonstrated active disease, and four patients demonstrated acute leukemia in high-risk remission. All achieved neutrophil engraftment a median of 17.5 days after transplantation with complete donor-type chimerism. The cumulative incidence of grades III to IV acute graft-versus-host disease was only 9%. Infection-related deaths were not observed. CD3+/CD4+ and CD3+/CD8+ T cells were strongly suppressed within 2 months after transplantation, but recovered on day 90. Relapse was observed in five of eight patients who underwent transplantation for active disease, whereas none of the three patients who underwent transplantation in first remission had a relapse.

Conclusions. We conclude that in vivo alemtuzumab enables haploidentical hematopoietic stem-cell transplantation without ex vivo graft manipulation.

Keywords: Alemtuzumab, T-cell depletion, HLA mismatch, Allogeneic hematopoietic stem-cell transplantation, Graft-versus-host disease.

(*Transplantation* 2005;79: 1351–1357)

Allogeneic hematopoietic stem-cell transplantation from a human leukocyte antigen (HLA)-identical sibling donor is an established treatment for hematologic malignancies. However, such a donor is available in only approximately 30% of patients in most developed countries (*1*, *2*). Therefore, alternative donor transplantation, including partially mismatched related donor transplantation, matched unrelated donor transplantation, and cord blood transplantation, has been investigated. Although transplantation from a one locus-mismatched related donor or a matched unrelated donor produces outcomes similar to those of transplantation from an HLA-identical sibling donor in high-risk patients (*3*), there is little chance of finding a one locus-mismatched related donor. In addition, it can sometimes be too time-consuming to coordinate a matched unrelated donor for patients with high-risk diseases. On the other hand, there is an excellent chance of identifying a family member who shares one haplotype with the patient and has two or three mismatched antigens in the second haplotype. Cord blood transplantation is also a possible alternative, but it is difficult to find a cord blood graft that contains enough nucleated cells for adult patients. Furthermore, it is impossible to obtain additional donor cells for immunotherapy after cord blood transplantation.

HLA incompatibility between the donor and recipient increases the risk of both graft rejection and severe graft-versus-host disease (GVHD). The outcome of two or three loci-mismatched transplantation without graft manipulation has been extremely poor (*3*, *4*), and thus it has been believed that ex vivo T-cell depletion from the graft is necessary to prevent severe GVHD. Although thorough T-cell depletion by CD34-positive cell selection has almost prevented GVHD (*5*), the incidences of graft rejection and infection increase after T-cell–depleted transplantation.

Campath-1 series of monoclonal antibodies is directed against human CD52, an antigen expressed on T, B, natural killer (NK), and dendritic cells, but not on hematopoietic stem cells (*6*, *7*). The original rat immunoglobulin (Ig)M and IgG monoclonal antibodies, Campath-1 M and Campath-1G, were used for ex vivo and in vivo T-cell depletion, respectively. The incidence of GVHD was significantly decreased by the use of these antibodies ex vivo only or both ex vivo and in vivo (*8–10*). Subsequently, Campath-1G was reshaped into a humanized form, alemtuzumab (Campath-1H), by genetic

This research was supported by a Grant-in-Aid for Scientific Research from the Ministry of Health, Labor, and Welfare.

Department of Cell Therapy and Transplantation Medicine, University of Tokyo Hospital, Tokyo, Japan.

Address correspondence to: Yoshinobu Kanda, M.D., Ph.D., Department of Cell Therapy and Transplantation Medicine, University of Tokyo Hospital, 7–3–1 Hongo, Bunkyo-ku, Tokyo 113–8655, Japan.

E-mail: ycanda-tky@umin.ac.jp.

Received 28 September 2004. Revision requested 11 November 2004. Accepted 15 December 2004.

ISSN 0041-1337/05/7910-1351

DOI: 10.1097/01.TP.0000158718.49286.14

engineering (*11*). It has a longer terminal half-life (15–21 days) than Campath-1G (<1 day) (*12*). The addition of in vivo alemtuzumab to a conditioning regimen decreases graft rejection by depleting host T cells. In addition, it prevents GVHD because the alemtuzumab concentration is higher than that required to kill donor T cells at the time of graft infusion and remains at a potentially lympholytic level for approximately 2 months after transplantation (*13*). In fact, Mackinnon and coworkers showed that in vivo alemtuzumab has excellent prophylactic action against GVHD in a reduced-intensity conditioning regimen using fludarabine, melphalan, and alemtuzumab followed by stem-cell infusion mainly from HLA-matched donors (*14*, *15*). However, there have been no reports on the application of in vivo alemtuzumab in two or three loci-mismatched transplantation. This study evaluates the safety of unmanipulated stem-cell transplantation from haploidentical two or three loci-mismatched related donors using alemtuzumab only in vivo.

PATIENTS AND METHODS

Patients

This study was approved by the ethical committee of the University of Tokyo Hospital, and all of the patients were seen and underwent transplantation at this hospital. Adult patients less than 65 years old who demonstrated high-risk acute leukemia, chemorefractory non-Hodgkin lymphoma, chronic myelogenous leukemia (CML) in blast crisis, myelodysplastic syndrome (MDS), or aplastic anemia with refractory severe neutropenia (<500/mm^3) were eligible for the study. The definition of high-risk acute leukemia included acute leukemia not in remission, in second or later remission, and in first remission with poor prognostic features such as positive Philadelphia chromosome (Ph$^+$), requiring more than two courses to achieve remission, and so on. Patients who had an available HLA-A/B/DR-matched or one locus-mismatched donor among family members were excluded. Patients who had an HLA-matched unrelated donor were also excluded unless the disease status precluded time-consuming donor coordination. Patients had to have a two or three loci-mismatched haploidentical related donor in good physical condition. Written informed consent was obtained from all patients and donors.

Stem-Cell Collection

Donors received granulocyte colony-stimulating factor at 200 μg/m^2 subcutaneously twice daily starting 3 days before the first collection of peripheral blood stem cells until the end of collection. Leukapheresis was performed daily until more than 5.0×10^6 CD34+ cells/kg of the recipient body weight were collected. Collected cells were then cryopreserved using standard techniques without ex vivo manipulation. The target cell dose was not achieved in three donors, but the minimum requirement dose had been set at 3.0×10^6 CD34+ cells/kg, and thus transplantation was performed using these grafts.

Conditioning Regimens

The conditioning regimen consisted of total body irradiation (TBI) at 2 Gy twice daily for 3 days (from days −7 to −5) and cyclophosphamide at 60 mg/kg per day for 2 days (from days −3 to −2). The dose of cyclophosphamide was decreased to 20 mg/kg per day for 2 days and etoposide at 40 mg/kg per day was added instead on day −4 in a patient with impaired cardiac function caused by anthracycline. For patients 50 years old or older, a non-TBI regimen consisting of fludarabine at 30 mg/kg per day for 6 days (days −8 to −3) and busulfan 1 mg/kg four times daily for 4 days (days −6 to −3) was applied. However, after we observed frequent relapse of lymphoid malignancies following this regimen, we added TBI at 2 Gy twice daily on day −1 and decreased the dose of busulfan to 4 mg/kg per day for 2 days (days −6 and −5) in the last two patients.

Alemtuzumab was added to these regimens at 0.2 mg/kg per day for 6 days (days −8 to −3). We adjusted the dose of alemtuzumab by body weight, because the body weight greatly differs among Japanese adult patients. The dose of daily alemtuzumab was determined by considering the total dose of alemtuzumab in previous studies (*14*, *15*), the average body weight of white patients, and the daily dose of alemtuzumab in pediatric studies (*16*). To prevent acute infusion-related reactions to alemtuzumab, patients were pretreated with 1 mg/kg of methylprednisolone. Alemtuzumab was infused over 4 hr. On the first day of alemtuzumab infusion, 3 mg of alemtuzumab was infused over 2 hr and, after confirming that no severe infusion-related toxicities were observed, we infused the remaining alemtuzumab over the next 2 hr.

Other Transplantation Procedures

On day 0, the cryopreserved donor cells were thawed and infused. Prophylaxis against GVHD was performed with cyclosporine A (CsA) and short-term methotrexate. CsA was started on day −1 at a dose of 3 mg/kg per day by continuous infusion, and the dose was adjusted to maintain a blood concentration between 250 and 350 ng/mL. CsA was changed to an oral form when it could be tolerated by the patient. Methotrexate was administered at 15 mg/m^2 on day 1 and 10 mg/m^2 on days 3, 6, and 11. For patients without acute GVHD, we started to taper CsA from day 30 by 10% per week and discontinued CsA on day 100.

Prophylaxis against bacterial, fungal, and Pneumocystis carinii infection consisted of tosufloxacin, fluconazole, and sulfamethoxazole/trimethoprim. Some of the patients who had active or recent aspergillosis received antifungal prophylaxis with micafungin instead of fluconazole. As prophylaxis against herpes simplex virus infection, acyclovir was given 500 mg/day intravenously or 1,000 mg/day orally from days −7 to 35, followed by long-term, low-dose (200 mg/day) oral administration (*17*). Patients without myeloid malignancies received granulocyte colony-stimulating factor (filgrastim) at 300 μg/day by 3-hr infusion beginning on day 10 until the neutrophil count recovered to 500/mm^3. Cytomegalovirus (CMV) antigenemia assay using C10/C11 antibody was performed at least once per week after engraftment. Ganciclovir was started when more than two positive cells were detected on two slides (*18*). Acute GVHD was graded as previously described (*19*). Patients who developed grades II to IV acute GVHD were treated with 1 mg/kg of intravenous methylprednisolone.

Host/donor cell chimerism after transplantation was analyzed by sex-chromosome FISH or the short tandem re-

TABLE 1. Patient characteristics

Median age	49.5 yr (range 27–60)	
Sex	Male 8/Female 4	
Diagnosis	ALL 5 (Ph^+ ALL 3), AML 2, MDS 2, CML-BC 1, NHL 2	
Disease status	Active disease	8
	High-risk remission	4
Comorbidities	Active/recent invasive aspergillosis	5
	Infective endocarditis, mitral valve replacement	1
	Anthracycline-induced cardiac failure	1
	Interstitial pneumonitis caused by radiation for breast cancer	1
	Diffuse lung infiltration of lymphoma	1
	Obstructive lung disease	1
	History of autologous transplantation	1
Donor	Sibling	4
	Son/daughter	6
	Uncle	1
	Cousin	1
No. of mismatched loci	Graft-versus-host direction 3 loci	7
	2 loci	5
	Host-versus-graft direction 3 loci	7
	2 loci	5
Conditioning regimen	Total body irradiation-based	6
	Fludarabine-based	6
Number of CD34+ cells in the graft	5.1×10^6 cells/kg (range 4.3–7.7)	
Number of CD3+ cells in the graft	2.6×10^8 cells/kg (range 1.8–7.1)	

ALL, acute lymphoblastic leukemia; AML, acute myeloblastic leukemia; MDS, myelodysplastic syndrome; CML-BC, chronic myeloid leukemia-blast crisis; NHL, non-Hodgkin lymphoma.

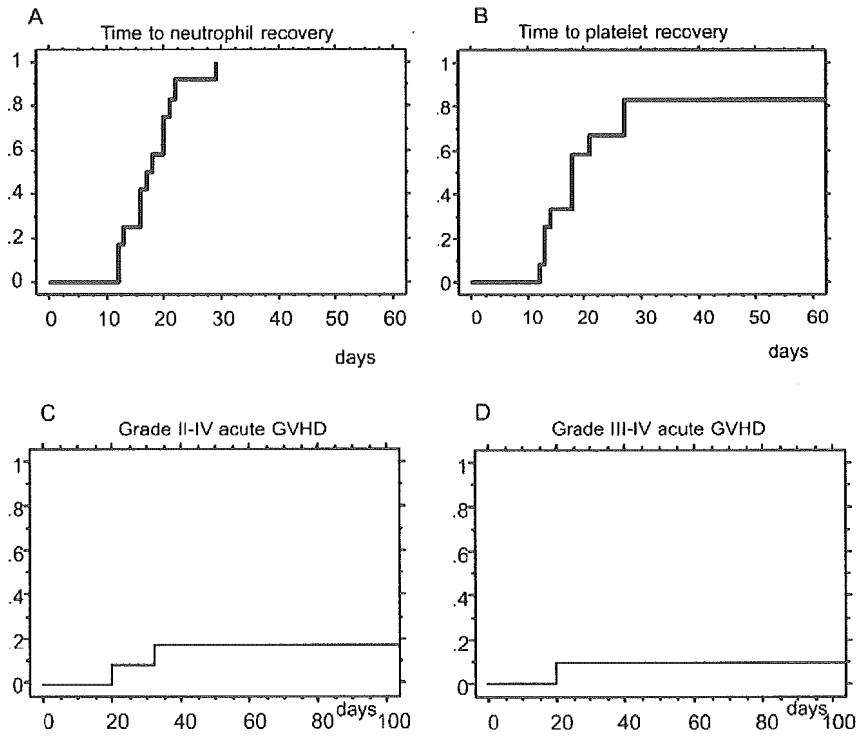

FIGURE 1. Days to neutrophil (A) and platelet (B) recovery and cumulative incidence of grades II to IV (C) and grades III and IV (D) acute GVHD after transplantation.

peat method monthly after transplantation (*20*). Immune reconstitution was evaluated by the quantification of CD3+/CD4+, CD3+/CD8+, CD3−/CD19+, and CD3−/CD56+ cells by flow cytometry. CMV-specific T-cell reconstitution was evaluated using fluorescent HLA-peptide tetramers in patients who were HLA-A*0201- or HLA-A*2402-positive

(*21*, *22*). As a functional assay, a phytohemagglutinin (PHA) stimulation test was performed as previously described (*23*).

Statistical Considerations

The primary endpoint of this study was the incidence of nonrelapse mortality within 100 days after transplantation. We defined success as the absence of early nonrelapse mortality and planned 7 and 9 patients in the first and second stages of this study, with target and lower success rates of 80% and 50% and alpha and beta errors of 10% and 10%, respectively (*24*). Nonrelapse mortality was observed in only one of the seven patients in the first stage, and thus the study was continued to the second stage. This was an interim analysis performed in February 2004. Overall survival and the incidences of GVHD and CMV reactivation were calculated using the Kaplan-Meier method. The data were compared with those who underwent allogeneic hematopoietic stem-cell transplantation from an HLA-identical sibling donor or a matched unrelated donor in the same period. Overall survival and the incidence of CMV reactivation were compared using the log-rank test. The recovery of immunologic parameters was compared using the Mann-Whitney *U* test.

RESULTS

Characteristics of the Patients

Twelve patients were included in the study (Table 1). There were eight males and four females with a median age of 49.5 years (range 27–60 years). The underlying disease was acute lymphoblastic leukemia (ALL) in five patients, acute myeloblastic leukemia in two patients, MDS in two patients, CML in blast crisis in one patient, and non-Hodgkin lymphoma in two patients. Eight patients demonstrated active disease at transplantation. The other four patients underwent transplantation for ALL in remission. Of these, two demonstrated Ph^+ ALL in first remission, one demonstrated ALL in second remission, and one demonstrated ALL in first remission and required more than 3 months to achieve remission. Most patients demonstrated comorbidities before transplantation including recent or active invasive aspergillosis in five, anthracycline-induced cardiac failure, interstitial pneumonitis caused by radiation for breast cancer, obstructive lung disease, and so on. Six patients who were more than 50 years old received a fludarabine-based regimen, whereas the other six received a TBI-based regimen.

Recovery of Donor Cells

The median number of CD34+ and CD3+ cells in the graft was 5.1×10^6 cells/kg (range 4.3–7.7) and 2.6×10^8 cells/kg (range 1.8–7.1), respectively. The median duration to the neutrophil recovery greater than 500/mm^3 and platelet recovery greater than 20,000/mm^3 without transfusion was 17.5 days (range 12–29 days) and 16 days (range 12–27 days), respectively (Fig. 1A and B). Complete donor-type chimerism was achieved on day 28 in all patients and was sustained thereafter, except for one patient who underwent transplantation for MDS (chronic myelomonocytic leukemia) using a fludarabine-based regimen and developed mixed chimerism (8.5% host cells) on day 60, and then relapsed with acute myeloblastic leukemia on day 90.

Graft-Versus-Host Disease

Grades II to IV acute GVHD was observed in two patients. One of the two patients developed grade II acute GVHD of the gut on day 32, which responded to methylprednisolone. The other patient developed grade III acute GVHD of the skin and gut on day 20, which was refractory to steroids, and eventually died of thrombotic microangiopathy on day 66. This patient received a three loci-mismatched graft from a cousin. He developed early hemorrhagic cystitis followed by postrenal azotemia and could not receive CsA at a therapeutic concentration. The cumulative incidence of grades II to IV and III to IV acute GVHD was 18% and 9%, respectively (Fig. 1C and D).

Of the eight evaluable patients who survived more than 100 days after transplantation, limited chronic GVHD that did not require treatment was observed in two patients. Notably, all five patients who are alive more than 100 days after transplantation as of this analysis are free from immunosuppressants.

Infectious Complications

Of the five patients who had recent or active invasive pulmonary aspergillosis before transplantation, one had a recurrence of aspergillosis during the neutropenic period after

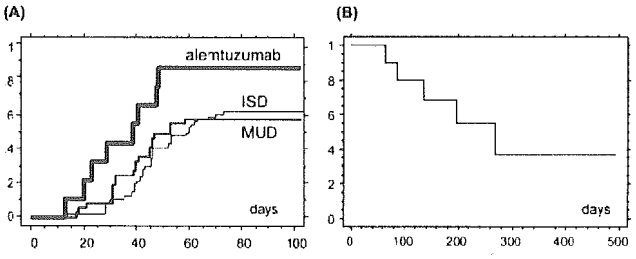

FIGURE 2. Cumulative incidence of cytomegalovirus reactivation detected by antigenemia assay, grouped according to the donor type (A). Overall survival of all patients (B). ISD, human leukocyte antigen (HLA)-identical sibling donors; MUD, matched unrelated donors.

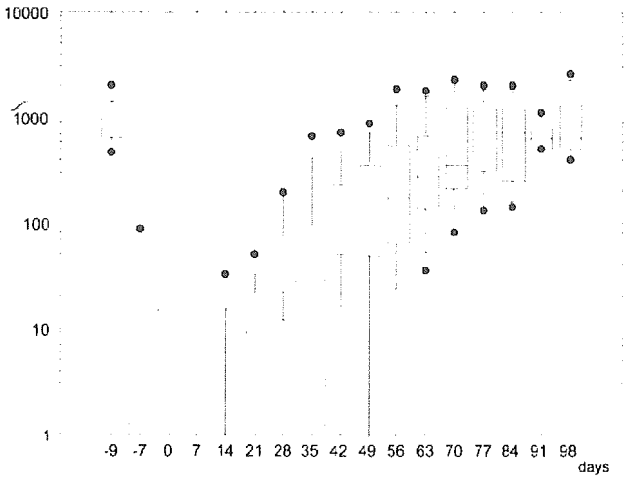

FIGURE 3. Recovery of peripheral blood lymphocytes after transplantation; 10, 25, 50, 75, and 90 percentile values (*box-and-whisker plot*). Outliers (*dots*).

transplantation, which was improved with neutrophil recovery. Otherwise, severe bacterial or fungal infection was not observed throughout the entire period after transplantation.

Of the 11 patients who were seropositive for CMV or who had a donor who was seropositive for CMV before transplantation, CMV reactivation was detected in 10 by antigenemia assay. The incidence of CMV reactivation was significantly higher than that after transplantation from an HLA-identical sibling donor or a matched unrelated donor (P=0.032, Fig. 2A). However, there was no death or severe disease related to CMV infection. Two patients developed asymptomatic CMV retinitis on days 149 and 160, respectively, and another patient developed hemorrhagic cystitis with CMV viruria on day 45, all of which were successfully treated with ganciclovir.

Relapse, Nonrelapse Mortality, and Survival

As a primary endpoint of the study, early nonrelapse mortality before day 100 was observed in one patient, who died of thrombotic microangiopathy and gut hemorrhage on day 66. Nonrelapse mortality was observed in another patient, who died of worsening of interstitial pneumonitis on day 197. This patient had received 60 Gy of local radiation to the right upper lung lobe for breast cancer and had already had local interstitial pneumonitis before transplantation. Six patients had a relapse of the underlying hematologic malignancy at a median of 111 days (range 49–223 days) after transplantation, and five of these had active disease before transplantation. Three of them died, and two are alive with disease. The remaining patient, who had undergone transplantation for ALL in second remission, received donor lymphocyte infusion after relapse of ALL and is alive in remission. None of the three patients who underwent transplantation for acute leukemia in first remission have relapsed thus far. Of these, two patients who had Ph^+ ALL were in molecular remission after transplantation. Overall survival is shown in Figure 2B.

Immune Reconstitution

The peripheral lymphocyte count dramatically decreased on the day after the first infusion of alemtuzumab and then gradually increased after day 28 (Fig. 3). Immune recon-

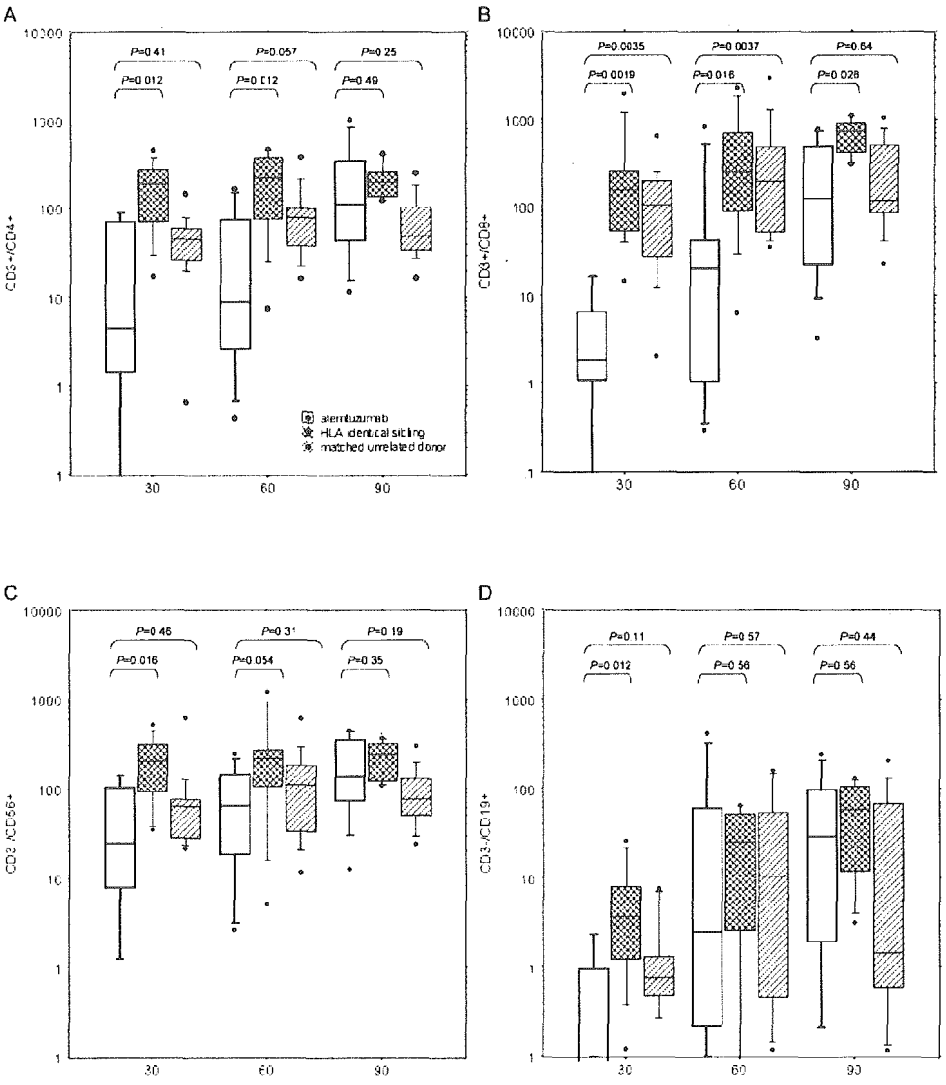

FIGURE 4. Recovery of CD3+/CD4+ (A), CD3+/CD8+ (B), CD3−/CD56+ (C), and CD3−/CD19(+) (D) cells on days 30, 60, and 90 after transplantation, grouped by the donor type; 10, 25, 50, 75, and 90 percentile values (*box-and-whisker plot*). Outliers (*dots*).